



Efficient coupling of light into and out of a photonic crystal waveguide via surface modes

Esteban Moreno^{a,*}, L. Martín-Moreno^b, F.J. García-Vidal^a

^a*Departamento de Física Teórica de la Materia Condensada, Facultad de Ciencias C-V,
Universidad Autónoma de Madrid, E-28049 Madrid, Spain*

^b*Departamento de Física de la Materia Condensada, ICMA-CSIC,
Universidad de Zaragoza, E-50009 Zaragoza, Spain*

Received 14 June 2004; received in revised form 19 July 2004; accepted 22 July 2004
Available online 20 August 2004

Abstract

In this paper, we show how the coupling of light into a photonic crystal waveguide can be greatly enhanced by creating a periodic modulation in the dielectric structure surrounding the entrance of the waveguide. In this way, surface modes supported by the system can funnel the light that impinges onto the surface into the interior of the waveguide. Moreover, we also demonstrate that the shape and direction of the beam that emerges from the structure can be tailored by constructing a periodic corrugation near the exit side of the waveguide.

© 2004 Elsevier B.V. All rights reserved.

PACS: 42.70.Qs; 78.20.Ci; 42.79.Ag

Keywords: Photonic crystals; Surface modes; Guided modes; Efficient couplers

1. Introduction

Photonic crystals (PhCs) offer unprecedented opportunities for moulding the flow of light [1]. In particular, light with a frequency lying within a photonic band gap (PBG) is prohibited from propagation along any direction inside a PhC [2,3]. Then, by introducing point and/or line defects in the crystal,

light can be guided inside the structure, opening the possibility of constructing very compact optical devices and circuits based on PhCs. In order to utilize such PhC circuits for actual applications, it is of paramount importance to find ways to couple them efficiently to traditional optical fibers. As the core size of a single mode conventional optical fiber is much larger than that of a PhC waveguide, it is very inefficient to directly connect an optical fiber to a PhC waveguide. The main strategy to surmount this problem has been the use of a dielectric wire waveguide located between the optical fiber and the PhC wave-

* Corresponding author. Tel.: +349 139 78515;
fax: +349 139 74950.

E-mail address: esteban.moreno@uam.es (E. Moreno).

guide [4,5]. Additionally, tapering of the waveguide junction helps to improve the coupling efficiency between the dielectric wire and PhC waveguides [6,7].

In this paper, we present an alternative way of enhancing the coupling of light into and out of a PhC waveguide by taking advantage of the surface electromagnetic (EM) modes that can be supported at the PhC's surfaces [8–10].

In recent years, it has been demonstrated [11,12] that the optical transmission through single subwavelength apertures made on optically thick metallic films can be greatly enhanced, if the aperture is flanked by periodic surface corrugations. Moreover, it has been also shown [11,13] that when the corrugation is placed at the output surface, light of appropriate wavelength can emerge from the structure as a collimated beam presenting an angular divergence of a few degrees. The physical origin of these enhanced transmission and beaming phenomena stems from the existence of surface EM modes (surface plasmons) decorating the interface between a metal and a dielectric. For frequencies within the PBG, the optical response of a PhC is analogous to the one associated with a metal. This fact, in addition to the existence of surface EM modes in PhCs with appropriate crystal termination surfaces, suggested that both enhanced transmission and beaming could also appear in PhCs. This hypothesis has been recently corroborated theoretically for both enhanced transmission and beaming phenomena [14], and experimentally verified for the case of beaming [15].

The aim of this paper is to analyze in more detail the enhanced transmission and beaming phenomena recently discovered in PhCs. The discussion is organized as follows: in Section 2, we present the prototype PBG system considered, together with an analysis of the surface modes supported by this structure. Section 3 describes the enhanced transmission phenomenon, whereas Section 4 presents our results for beaming effects.

2. Two-dimensional PBG and surface modes

All results presented in this paper have been obtained with a frequency-domain computational technique [16,17], based on the multiple multipole (MMP) method [18]. In Section 4, this computational scheme

is used for the accurate modelling of PhC waveguide discontinuities [17], whereas in Section 2, we show the application of the technique for the calculation of the surface modes supported by a given PhC surface termination. The determination of the band structure corresponding to these surface modes is performed with a generalization of the method discussed in [16] and has not been described before. The main computational novelty here is that the employed supercell is periodic only along the mode propagation direction (i.e., parallel to the crystal interface) and it is open along the orthogonal direction. Related ideas have been applied in the context of PhC guided modes [19].

For proof of principle purposes, we consider as the PBG system a two-dimensional square array of infinitely long dielectric cylinders ($\epsilon = 11.56$) of radius $r = 0.18a$, where a is the lattice constant (Fig. 1a). For the chosen set of geometrical and dielectric parameters, the structure presents a PBG for reduced frequencies $\omega a/2\pi c$ in the range (0.30, 0.44) (see the projected band structure in Fig. 2). This PBG only appears for E polarized light (electric field pointing along the axis of the cylinders). As demonstrated in [8], the regular termination of this PhC does not support surface modes. In the literature, surface states are typically created by cutting the outer part of the interface cylinders, thus leaving a monolayer of hemicylinders [9]. Here, we show that a surface state can

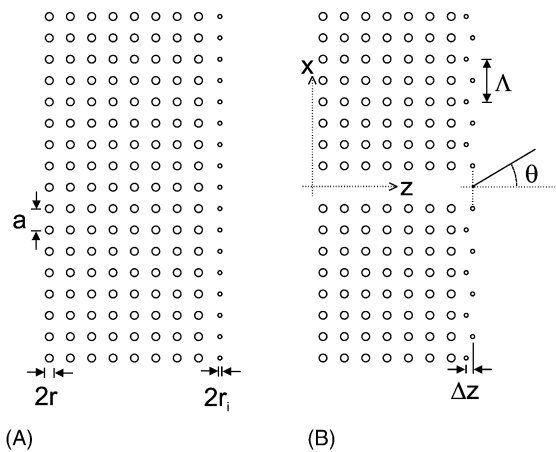


Fig. 1. Schematics of the considered structures. (a) Parameters of the crystal bulk and of the interface supporting surface modes. The cylinders at the rightmost monolayer have a radius different from that in the bulk. (b) Parameters for the case with a PhC waveguide and a corrugated interface.

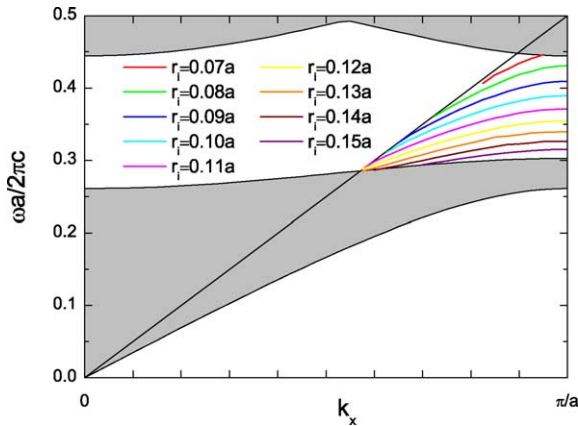


Fig. 2. Dispersion relation curves of the surface modes supported by the analyzed structure for various values of the radius r_i of the interface cylinders. Frequency is expressed in reduced units ($\omega a/2\pi c$). The shaded areas depict the projected band structure of the bulk crystal. The black line is the vacuum light line.

also be created by just decreasing (or increasing) the radius r_i of the cylinders at the interface monolayer (Fig. 1a). Incidentally, this procedure may be advantageous from a technological point of view. In Fig. 2, the dispersion relation of the induced surface modes is plotted for different values of r_i ranging from $0.07a$ (upper PBG limit) to $0.15a$ (lower PBG limit). The surface bands are located inside the PBG and outside the light cone. Notice that, as expected, the group velocity of these modes at $k_x = \pi/a$ is equal to zero; we will comment further about this point below.

3. Enhanced coupling of light into a PhC waveguide

As mentioned in the introduction, we are interested in taking full advantage of the surface modes supported by the structure in order to enhance the coupling of light into a PhC waveguide. A waveguide is built in our structure by removing just one row of cylinders in the z direction (Fig. 1b). It is worth noting that, for the enhanced transmission studied in Section 3, a finite structure is considered (slab thickness: eight layers, lateral extension: $40a$). Fig. 3 shows (green line) the transmittance spectrum for a normally incident plane wave for the case in which the radius of the cylinders at the interface layers is $r_i = r = 0.18a$ (no

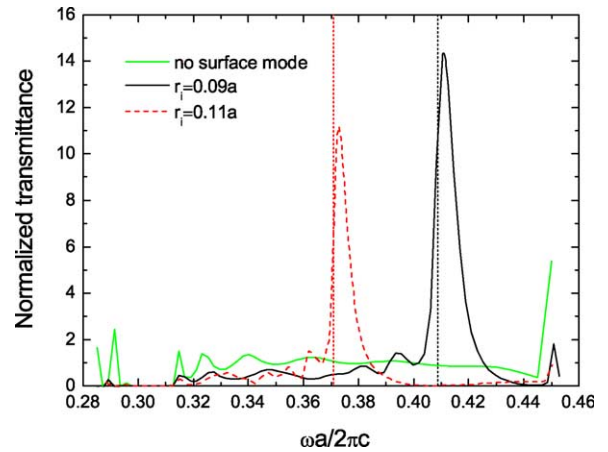


Fig. 3. Normalized transmittance through the PhC waveguide as a function of the reduced frequency. Green curve: standard interface in which no surface mode is present; black curve: interface made of cylinders with radius $r_i = 0.09a$; red-curve: interface made of cylinders with radius $r_i = 0.11a$. In these two last cases the interface is corrugated, the number of indentations is $N = 9$, and the depth of the modulation is $\Delta z = -0.3a$. Vertical lines mark the locations of the frequencies of the surface modes at $k_x = \pi/a$ (see Fig. 2), corresponding to the cases $r_i = 0.09a$ and $0.11a$. The normalization employed is explained in the text. (For interpretation of the references to color in this figure legend, the reader is referred to the web version of the article.)

surface mode present). The transmittance through the PhC waveguide is normalized to the power impinging onto a length a . As can be seen in this figure, the spectrum is rather uniform (around 1) inside the frequency gap with some oscillations, due to the excitation of some standing wave resonances present in our finite system. The region of zero transmittance around 0.30 – 0.31 is simply due to the lack of a guided mode for these frequencies.

If the radii of the input interface cylinders is decreased, eventually the PhC interface supports a surface mode. Even in this case, the transmission spectra do not change significantly with respect to the previous case. The reason is simple: the surface modes displayed in Fig. 2 are truly surface states that do not couple to radiative modes (they live outside the light cone). As also happens in the metallic case, a periodic modulation of the PhC surface is needed to allow the coupling of the continuum of radiative modes in vacuum to the surface modes supported by the system. In this way, a reciprocal lattice vector of the superimposed lattice can be added to the parallel

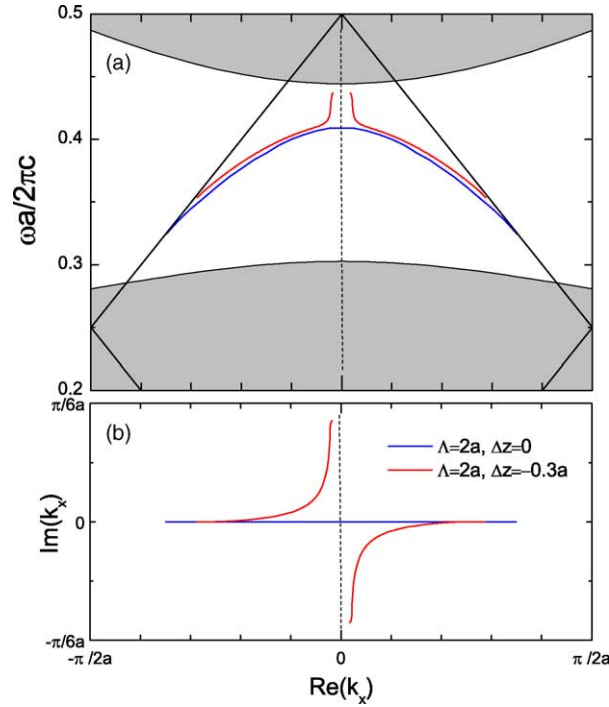


Fig. 4. (a) Dispersion relation curves, ω in reduced units vs. $\text{Re}(k_x)$. Red curve: periodically modulated interface with $r_i = 0.09a$, $\Lambda = 2a$ and $\Delta z = -0.3a$. Blue curve: un-modulated case ($\Delta z = 0$) but with supercell periodicity $2a$. (b) $\text{Im}(k_x)$ vs. $\text{Re}(k_x)$ for the modes plotted in the upper panel. (For interpretation of the references to color in this figure legend, the reader is referred to the web version of the article.)

wavevector of the surface mode, folding the mode dispersion curve into the light cone. In other words, surface modes become leaky surface modes. The associated parallel momenta, k_x , of these surface resonances have an imaginary component, reflecting the fact that when the resonance propagates along the surface, part of its energy is re-radiated. In the present case, the superimposed interface corrugation can be achieved, e.g., by shifting in the z -direction every second cylinder, thus obtaining a corrugation period $\Lambda = 2a$ (see Fig. 1b). In Fig. 4, we show the dispersion relation of the surface bands for the case in which $r_i = 0.09a$ and the corrugation period is $\Lambda = 2a$ with a corrugation depth $\Delta z = -0.3a$. In panel (a) of Fig. 4, we plot ω versus $\text{Re}(k_x)$; whereas, panel (b) renders $\text{Im}(k_x)$ versus $\text{Re}(k_x)$. The behavior of the complex band (red curve) for very small k_x values (not plotted) is involved and is currently under investigation.

It is now interesting to analyze the consequences of the periodic modulation of the surface on the transmittance spectrum. In Fig. 3, we plot the normalized

transmittance versus frequency for two different modulated interfaces corresponding to $r_i = 0.09a$ (blue curve) and $r_i = 0.11a$ (red curve). In both cases, the modulation period is $\Lambda = 2a$, the number of indentations is $N = 9$ and the modulation amplitude is $\Delta z = -0.3a$. The vertical dashed lines correspond to the frequencies of the surface modes at $k_x = \pi/a$ in the un-modulated surfaces (see Fig. 2). It is clear that the periodic modulation of the surface surrounding the waveguide entrance provokes the appearance of the resonant transmission peaks and there is a close correspondence between the location of these peaks and the corresponding frequencies of the surface modes at $k_x = \pi/a$. The mechanism proposed in the previous paragraph is thus confirmed. The fact that the peaks' frequencies do not exactly agree with the dashed vertical lines can be ascribed to the following. The frequency of the surface bands of the non-corrugated surface depends not only on the radius of the interface cylinders (as shown in Fig. 2), but also on the distance between the line of interface cylinders and the

next line of cylinders inside the crystal. We have verified that when all interface cylinders are shifted towards the inner part of the crystal, the band frequency increases. Therefore, it is clear that the corrugation must also shift the band frequency, since it amounts to displacing $\Delta z = -0.3a$ every second cylinder.

Since the surface mode frequency at the $k_x = \pi/a$ point can be tuned to every possible frequency within the PBG (see Fig. 2), the enhanced transmission can also be tuned to every frequency within the PBG (except where the PhC waveguide does not support a guided mode). The peak value for the case $r_i = 0.09a$ is 14, which means that the energy flux collected into the PhC waveguide corresponds to the one impinging in a cross-section around $14a$. We are currently investigating how this effective cross-section could be increased by considering a shallower corrugation with a larger number of periods. In order to illustrate the funnel effect associated to the excitation of the surface resonance, Fig. 5 displays the Poynting field modulus for a frequency $\omega a/2\pi c = 0.408$ for the particular case $r_i = 0.09a$, $\Lambda = 2a$, $N = 9$, and $\Delta z = -0.3a$. The excitation of a surface resonance covering a region of around $14a$ is clearly evident in this picture.

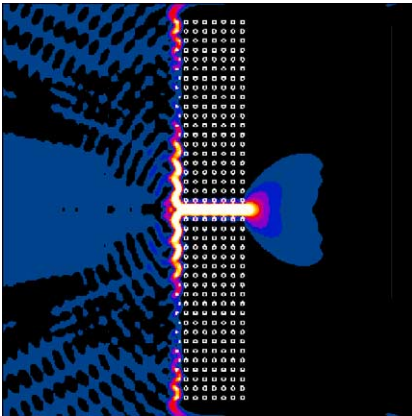


Fig. 5. Poynting field modulus $S(z, x)$ for the case in which a normally incident plane wave is impinging from the left. The reduced frequency of the incident light is 0.408, that corresponds to the location of the surface mode at $k_x = \pi/a$ for $r_i = 0.09a$. The number of indentations is $N = 9$ and the depth of the modulation is $\Delta z = -0.3a$.

4. Beaming light from a photonic crystal waveguide

In the case of structured metals, it has been reported [11–13] that when the periodic corrugation is placed at the exit interface instead at the input, beaming effects appear for the resonant frequency in which enhanced transmission was obtained when the periodic corrugation was built around the input interface. We now show this is also the case for PhC waveguides.

Fig. 6 displays the far-field radial component of the Poynting vector field radiated out of a PhC waveguide, surrounded by various kinds of corrugations as a function of azimuthal angle θ (θ is defined in Fig. 1b). The structure is fed with a guided mode running along a semiinfinite PhC waveguide. For comparison purposes the cases with no surface mode ($r_i = 0.18a$, green curve) and with non-radiative surface mode ($r_i = 0.09a$, light blue curve) are shown. In these two cases, no beaming is observed, as it should occur

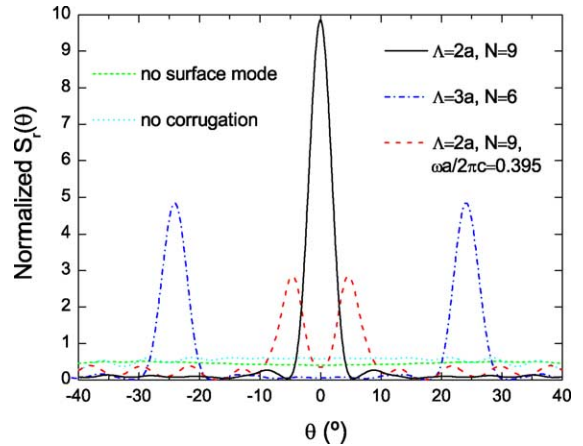


Fig. 6. Far-field radial component of the Poynting vector, radiated out of a PhC waveguide as a function of the azimuthal angle, θ . In all cases displayed, the integral in θ of the angular transmission distribution, $rS_r(\theta)$, is normalized to unity. The green curve corresponds to the standard interface and the light blue curve to the case in which a surface mode is supported for $r_i = 0.09a$, but no corrugation is present. The black line shows the distribution for a modulated surface with $\Lambda = 2a$, $N = 9$ and $\Delta z = -0.3a$; whereas, the dark blue curve corresponds to $\Lambda = 3a$, $N = 6$ and also $\Delta z = -0.3a$. In all previous cases, the reduced frequency of light is 0.408. The red curve displays the angular transmission distribution with the same geometrical parameters of the black curve, but for a slightly different frequency, 0.395, in reduced units. (For interpretation of the references to color in this figure legend, the reader is referred to the web version of the article.)

for a waveguide opening with size of the order of the radiated wavelength in vacuum. The remaining curves correspond to leaky modes with $r_i = 0.09a$. The black curve is the case with reduced frequency 0.408, and $\Lambda = 2a$. As seen in Fig. 2, these r_i and ω correspond to $k_x = \pm\pi/a$. In first order coupling, the superimposed corrugation allows one to add a grating momentum $K = \mp 2\pi/\Lambda = \mp \pi/a$. Therefore, the surface state is coupled to radiation with zero parallel momentum, i.e., radiation that propagates in the $\theta = 0^\circ$ direction. If the corrugation has a period $\Lambda = 3a$ (every third cylinder is shifted, dark blue curve), the added grating momentum is $K = \mp 2\pi/(3a)$. It is easy to verify that the corresponding radiation angle should be $\theta = 24^\circ$, as confirmed by the simulation. If the system is operated at a slightly lower frequency, 0.395 (red curve) the photon travelling along the surface has a lower momentum. By keeping $\Lambda = 2a$, the addition of the grating momentum produces a photon with non-zero parallel momentum, corresponding to two beams at $\theta \neq 0^\circ$.

Let us recall that for the cases with frequency 0.408, $r_i = 0.09a$, the mode's group velocity is zero (Fig. 2). One may wonder how is it possible that a mode that does not carry power gives rise to such a wealth of phenomena as those described in the present and previous sections. The answer can be found in Fig. 4. It is true that the non-corrugated surface does support a standing wave at the mentioned frequency, but this behavior changes as soon as the interface is corrugated, obtaining a non-zero slope for the dispersion curve. In this way the photons propagate with non-zero speed along the interface, interact with the corrugations, and finally radiate. As a consequence, the effective size of the waveguide opening is increased and this mechanism allows one to obtain collimated beams, thus circumventing the diffraction limit.

In conclusion, a new approach for efficient coupling to and from PhC waveguides has been presented. The mechanism relies on the excitation of surface modes at the PhC interface. The surface state modal wavelength can be controlled by tuning the geometrical parameters of the interface cylinders. The coupling between radiative modes and surface modes is, in turn, achieved by superimposing an additional periodicity to the PhC interface. If the corrugation is located at the input interface, the proposed structure

can be used to funnel light from the vacuum inside the waveguide; whereas, corrugation at the output interface will collimate, within a few degrees, the light exiting from a PhC waveguide.

Acknowledgements

Financial support by the Spanish MCyT under contracts MAT2002-01534 and MAT2002-00139 is gratefully acknowledged.

References

- [1] J.D. Joannopoulos, R.D. Meade, J.N. Winn, *Photonic Crystals: Molding the Flow of Light*, Princeton University Press, Princeton, NJ, 1995.
- [2] E. Yablonovitch, *Phys. Rev. Lett.* 58 (1987) 2059.
- [3] S. John, *Phys. Rev. Lett.* 58 (1987) 2486.
- [4] A. Adibi, Y. Xu, R.K. Lee, A. Yariv, A. Scherer, *J. Lightwave Technol.* 18 (2000) 1554.
- [5] E. Miyai, M. Okano, M. Mochizuki, S. Noda, *Appl. Phys. Lett.* 81 (2002) 3729.
- [6] Y. Xu, R.K. Lee, A. Yariv, *Opt. Lett.* 25 (2000) 755.
- [7] A. Mekis, J.D. Joannopoulos, *J. Lightwave Technol.* 19 (2001) 861.
- [8] R.D. Meade, K.D. Brommer, A.M. Rappe, J.D. Joannopoulos, *Phys. Rev. B* 44 (1991) 10961.
- [9] J.N. Winn, R.D. Meade, J.D. Joannopoulos, *J. Mod. Opt.* 41 (1994) 257.
- [10] F. Ramos-Mendieta, P. Halevi, *Phys. Rev. B* 59 (1999) 15112.
- [11] H.J. Lezec, A. Degiron, E. Devaux, R.A. Linke, L. Martin-Moreno, F.J. Garcia-Vidal, T.W. Ebbesen, *Science* 297 (2002) 820.
- [12] F.J. Garcia-Vidal, H.J. Lezec, T.W. Ebbesen, L. Martin-Moreno, *Phys. Rev. Lett.* 90 (2003) 213901.
- [13] L. Martin-Moreno, F.J. Garcia-Vidal, H.J. Lezec, A. Degiron, T.W. Ebbesen, *Phys. Rev. Lett.* 90 (2003) 167401.
- [14] E. Moreno, F.J. Garcia-Vidal, L. Martin-Moreno, *Phys. Rev. B* 69 (2004) 121402(R).
- [15] P. Kramper, M. Agio, C.M. Soukoulis, A. Birner, F. Müller, R.B. Wehrspohn, U. Gsele, V. Sandoghdar, *Phys. Rev. Lett.* 92 (2004) 113903.
- [16] E. Moreno, D. Erni, Ch. Hafner, *Phys. Rev. B* 65 (2002) 155120.
- [17] E. Moreno, D. Erni, Ch. Hafner, *Phys. Rev. E* 66 (2002) 036618.
- [18] Ch. Hafner, *Post-Modern Electromagnetics*, John Wiley and Sons, Chichester, 1999.
- [19] J. Smajic, Ch. Hafner, K. Rauscher, D. Erni, in: *Proceedings of Progress in Electromagnetics Research Symposium (PIERS 2004)*, March 28–31, Università di Pisa, Pisa, 2004 pp. 21–24.